RESEARCH ARTICLE

Impact of Carboxymethylation of *Albizia procera* Gum on Rheological Changes and Drug Release from Matrix Tablets

Sudipta Mukherjee*, Biswanath SA, Jasmina Khanam, Sanmoy Karmakar, Rudranil Bhowmik

Department of Pharmaceutical Technology, Division of Pharmaceutics, Jadavpur University, Kolkata, West Bengal, India.

Received: 05th August, 2022; Revised: 03rd September, 2022; Accepted: 21st January, 2023; Available Online: 25th June, 2023

ABSTRACT

The use of carbohydrate polymers in pharmaceutical formulations as drug delivery carriers has gained significant interest from many perspectives. As an exudate of the *Albizia* tree, *Albizia procera* (Mimosaceae), a carbohydrate polymer, is used as an excipient to develop sustained-release drug delivery systems, owing to its biocompatibility and biodegradability. This study was conducted to investigate the influence of carboxymethylation of *A. procera* gum on rheological properties and drug release from the matrix tablet formulations. The study also revealed the comparative characterization of the native form of *A. procera* (NAP) as well as the carboxymethylated *A. procera* (CMAP). The rheological assessments of both polymers under different pH divulged the flow behavior, linear viscoelasticity (LVE), structural deformation, and gel network formation. The drug release from NAP and CMAP matrices of various formulations were evaluated and established correlations with rheology.

Keywords: *Albizia procera*, Carboxymethylation, Rheology, Amplitude sweep, Frequency sweep, Damping factor

International Journal of Drug Delivery Technology (2023); DOI: 10.25258/ijddt.13.2.15

How to cite this article: Mukherjee S, Biswanath SA, Khanam J, Karmakar S, Bhowmik R. Impact of Carboxymethylation of *Albizia procera* Gum on Rheological Changes and Drug Release from Matrix Tablets. International Journal of Drug Delivery Technology. 2023;13(2):551-561.

Source of support: Nil.

Conflict of interest: None

INTRODUCTION

Natural polymers (hydrophilic and hydrophobic) have been extensively used to fabricate NDDS for the past several years, resulting in substantial growth in the applications of these polymers. There are several species of *Albizia procera*, and one of these is considered fast-growing, semi-deciduous, light-demanding, relatively drought-tolerant, and susceptible to roots sucking after damage. It is locally named safed siris, karanji, Dun-siris, and forest siris in India. Species in the *Albizia* genus belong to the Fabaceae family, subfamily Mimosoideae. *A. procera* is found in a variety of tropical types of forests, including tropical semi-evergreen forests, tropical moist deciduous forests, low alluvial Savannah woodlands, and northern subtropical broadleaved forests throughout its range.[1] In Vietnam, it is found in tropical rainforests, dry open forests, and savannas.[2] Many studies have found that *A. procera* gum contains β-(1→3)-D-galactopyranose units with some β-(1→6)-D-galactopyranose units[3] and α-(1→3)-L-arabinofuranose units.[4-7]According to certain studies, the two primary monosaccharides of the hydrolyzed *A. procera* gum are galactose and arabinose.[3] The linkage and monosaccharide components in a gum's structure can influence its rheological and functional properties.[4-7] The customization of the D-galactopyranose units by chemical modification[8] and cross-linking[9] may result in changes in the rheological stability of *Albizia* gum that may lead to variation in diffusivity for drug delivery systems.[10] Rheological characterization is a potential measure to determine the mechanical strength[11] of a polymeric matrix that influences the drug release pattern from delivery systems.[12] The study and measurement of variable rheological moduli can predict drug diffusion from the entangled polymeric matrix.[13] The approach is aimed at investigating and studying the stability of polymers under the linear visco-elastic regime that greatly impacts drug release from the systems.

MATERIALS AND METHOD

Materials

Pulverised native *A. procera* (NAP) gum was procured from the University of Mizoram (Mizoram, India). Sodium hydroxide, hydrochloric acid, monochloroacetic acid (99.0%), trisodium phosphate dodecahydrate (mol.wt 380.119 g/mol), and trisodium citrate were obtained from Loba Chemie Pvt. Ltd (Mumbai, India). Methanol of the analytical reagent grade (99% v/v) was purchased from Merk Specialty Pvt. Ltd. (Mumbai, India). All other analytical-grade chemicals

*Author for Correspondence: dipta07tech@gmail.com

and reagents were purchased from commercial sources. Metformin was provided as a drug sample by Stadmed Pvt. Ltd. Kolkata, India.

Carboxymethylation of *A. procera*

The base-catalyzed reaction was used for the carboxymethylation of NAP. The powdered NAP was sieved through 45 meshes and weighed. A creamy dispersion was prepared by slowly sprinkling powdered NAP (10 g) into an aqueous sodium hydroxide solution (45% w/v). The mixture was kept in a double-walled ice chamber (stainless steel) at a temperature of 0 to 8°C and stirred vigorously to achieve proper hydration. At a temperature between 15 to 18°C, a slow, steady addition of monochloroacetic acid (45% w/v) was made to the slurry. The mixture was stirred continuously and allowed to react for a while. In order to complete the reaction, the mixture was heated at 75°C in a water bath for one hour while being stirred regularly and kept at room temperature for 24 hours. Afterward, the resultant mass was precipitated with aqueous methanol (80% v/v) and filtered through 8 mm filters. After collecting the filtered cake, it was air-dried and washed several times with aqueous methanol (80% v/v). The pH of CMAP was adjusted to neutral using glacial acetic acid and then washed with pure methanol. The tiny semi-crystalline CMAP was air-dried and kept in a hot oven at 60°C for 24 hours.

Characterization of CMAP

Degree of substitution (D_S)

Approximately 500 mg of CMAP was added to 5 mL of aqueous methanol (80% v/v) and stirred to form a dispersion. To this dispersion, concentrated HCl was added and stirred for 3 hours. Afterward, the mixture was filtered and the residue was washed with aqueous methanol (80% v/v) until neutrality was achieved with litmus papers. After a final wash with pure methanol, the sample was dried. 200 mg of dried CMAP was weighed accurately and added to 1.5 mL of aqueous methanol (70% v/v). Within a few minutes, 20 mL of distilled water was added to the mixture, followed by the addition of 5 mL of 0.5 N NaOH solution. A shaker was used to shake the mixture for 3 hours in order to dissolve the sample. The solution was titrated with 0.4 N HCl using phenolphthalein as an indicator.[14] The following equation was used to determine the O-carboxymethyl group's substitution degree.[15]

$$Ds = \left[\frac{0.162\ A}{1 - 0.058A}\right] \quad (1)$$

Where, A represents the milli-equivalents of NaOH required per gram of sample.

FTIR spectrum analysis

Finely powdered samples of NAP and CMAP were mixed individually with dried potassium bromide (1:100) in a mortar, followed by pelletization in a hydraulic press at a pressure of 400 kg cm^{-2}. The pellets were analyzed for FTIR spectra using FTIR spectrophotometer (Perkin Elmer, RX-1, UK), in the range from 4000–400 cm^{-1}.

Differential scanning calorimetry study

DSC thermograms for NAP and CMAP were obtained using a DSC-4000, Perkin-Elmer, United States. An aluminum pan was used to seal the samples, and the samples were heated between 30 and 300°C at a rate of 10°C/minute.

Solid-state ^{13}C-NMR spectroscopy

The solid state ^{13}C-NMR study was conducted using each 300 mg of powdered samples of NAP and CMAP on an NMR spectrometer (JEOL, Japan) at field strength of 400 MHz using a cross-polarization method.

X-ray diffractometer

The XRD of powdered samples of NAP and CMAP were recorded using an X-ray diffractometer (ULTIMAIII, Rigaku, Japan). At a voltage of 40 kV and a current of 30 mA, an X-ray generator was operated, with the K-β filtered Cu radiation at 1.54056 Å as the source of radiation. The powdered specimens were scanned at a 3°/min speed from 5 to 80° diffraction angle (2θ).

Zeta potential measurements

The zeta potential measurements were carried out in a Zeta-sizer (Nano ZS90, Malvern Instruments Ltd., UK) using 1% (w/v) dispersion of NAP and CMAP at neutral pH. This study used deionized water as a dispersion medium and several disposable zeta cells (DTS 1070) for each sample at 25ºC. The experiments were repeated three times, with the mean values reported in this study.

Rheological studies

Rheological experiments were conducted in the present study using a Modular Compact Rheometer (MCR 102, Anton Parr, Austria). In the experimental setup, a standard 1° cone geometry (CP - 40) with a diameter of 40 mm was used.

Rheological analyses were performed on the polymer solutions (5% w/v) of NAP and CMAP prepared in various media that slowly turned into matrix solutions. For each polymer, three types of matrices were prepared at different pH levels to investigate the effects of pH on viscosity. The matrices under the "Polymer-A" category (NAP-A, CMAP-A) were prepared by dissolving the required amount of polymer in an acidic solution with constant stirring at 60ºC. The pH of the matrices was adjusted to 1.2 at room temperature using a 0.2 (M) HCl solution. Similarly, "polymer-B" matrices (NAP-B, CMAP-B) were prepared for each polymer in buffer solution and the pH was adjusted to 6.8 with a 0.2 (M) NaOH solution. For "Polymer-W" category matrices (NAP-W, CMAP-W), deionized water was used to maintain neutral pH (pH 7).

A dynamic rotation mode (flow curve) and an oscillatory mode were used to perform the tests. The dynamic rotational mode was used to study changes in viscosity caused by variable shear rates in the samples.

The oscillatory mode was employed for the polymers to study the amplitude sweep and frequency sweep against loss and storage moduli (G' and G"). The amplitude sweep was carried out at a fixed angular frequency (ω=6.2831853 rad/sec)

Table 1: Tablet formulations

Sl no.	*Ingredients*	*Quantity (mg) per tablet of each formulation*									
		F1	*F2*	*F3*	*F4*	*F5*	*F6*	*F7*	*F8*	*F9*	*F10*
1	MET	250	250	250	250	250	250	250	250	250	250
2	NAP	250	450	550	650	750	-	-	-	-	-
3	CMAP	-	-	-	-	-	250	450	550	650	750
4	Lactose anhydrous	500	300	200	100	50	500	300	200	100	50
5	MCC	80	80	80	80	30	80	80	80	80	30
6	Purified water	Qs*	Qs	Qs	Qs	Qs	Qs	Qs	Qs	Qs	Qs
7	Magnesium stearate	20	20	20	20	20	20	20	20	20	20

*Qs denote sufficient quantity

where the strain (γ=0.01–10%) was varied to produce structural deformation on the entangled polymer.

The frequency sweep was carried out to study the changes in G' and G" against variable angular frequency (ω =0.1–10 rad/sec) using the pre-determined strain (%) under the linear viscoelastic (LVE) regime from amplitude sweep.

Drug-polymer DSC Compatibility Study

A differential scanning calorimeter (DSC-4000, Perkin-Elmer, USA) was used to record the DSC thermograms of the physical mixtures of MET with NAP and CMAP. The samples were impenetrably sealed inside an aluminum pan and heated from 30 to 300°C under a nitrogen atmosphere (20 mL/min) at a scan rate of 10°C/min.

Preparation of Matrix Tablet

Metformin hydrochloride (MET) as the active ingredient, powdered NAP and lactose and microcrystalline cellulose (MCC) were separately passed through the sieve with mesh #40. In the weight ratio shown in Table 1, the drug was thoroughly mixed (dry mixing) with the polymer and other ingredients for 15 minutes. The powder mixture was then moistened with the appropriate amount of purified water to form a moist cohesive mass. The cohesive mass was screened through a sieve with mesh #16, and the resulting moist granules were dried in a tray dryer at 65°C until the moisture content reached 2% w/v. The dried granules were passed through the sieve with mesh size 20 of BS, lubricated with magnesium stearate (2% w/w). The lubricated granules were compressed into tablets on a tablet compression machine (RIMEK, Karanavati Engineering Ltd., Gujarat, India) using 19.5 mm of oval concave surface punch. The compression force was adjusted to obtain tablets with hardness in the range of 49.04 to 63.74 Newton. MET contains CMAP tablets were prepared in a similar manner.

Physical Characterization of Tablet

Uniformity of weight

The test was carried out in accordance with the official procedure.[16] The weight variation of 20 tablets of each formulation was studied using an electronic balance (Precisa, XB600 M-C, Switzerland). The tablets were selected at random and weighed individually. Individual weights (X_1, X_2, ..X_{20}) were compared to the average weight of the tablets.

$$\text{Average weight (X)} = \left[\frac{X_1+X_2+X_3+\ldots+X_{20}}{20}\right] \quad (2)$$

Crushing strength and friability

The crushing strength and friability of 20 tablets for each formulation were determined using the Monsanto hardness tester (Cadmach, Ahmedabad, India) and the Roche friability (Campbell Electronics, Mumbai, India), respectively. To determine the percentage of weight loss, the friability was rotated at 25 ± 1 rpm for 4 minutes, and then the tablets were de-dusted and weighed again.

Content uniformity test

A fine powder was prepared by weighing and grinding 20 tablets. The powder containing about 0.1 g of metformin hydrochloride was precisely weighed and shaken for 15 minutes with 70 mL of water then diluted with water to 100 mL and filtered. From the filtrate, 10 mL was diluted to 100 mL with water, and then 10 mL from that dilution was diluted to 100 mL with water. Using a double-beam spectrophotometer (Shimadzu, UV, 2450, Japan), the absorbance of the resulting solution (0.01 mg/mL) was determined at 232 nm. The content of $C_4H_{11}N_5$, HCl was calculated by using 798 as the specific absorbance at 232 nm.[17]

Drug Release Study

Using a USP II tablet dissolution tester (Electrolab, TDP-06P, India), matrix tablets were tested for in-vitro drug release in acidic (pH 1.2) and phosphate buffer solutions (pH 6.8). In a cylindrical dissolution vessel (1000 mL) with a stirring speed of 100 rpm, 750 mL of 0.1M hydrochloric acid solution was kept at 37 ± 0.5ºC. Then a randomly selected tablet from each formulation was placed inside it. During the experiment, aliquots were drawn every hour and promptly replaced with the same volume of fresh medium maintained at 37 ± 0.5ºC. After 2 hours of dissolution in acidic medium, 250 mL of 0.2M trisodium phosphate dodecahydrate solution (previously maintained at 37 ± 0.5ºC) was added. The medium was adjusted to a pH of 6.8 ± 0.05 with 2M sodium hydroxide solution.

The dissolution was carried out for 12 hours. The aliquots obtained by filtration and appropriate dilution were analyzed spectrophotometrically. The amount of drug released was measured at the wavelength of maximum absorbance (λ_{max}) in the relevant medium. MET exhibited maximum absorbances at 232 and 230 nm in acidic and buffer solutions, respectively.

RESULTS AND DISCUSSION

Extent of Carboxymethylation

The native *A. procera* gum is primarily composed of galactose and arabinose.[3] Structurally, NAP consists of a linear chain of - (1→ 3)-β-D-galactopyranose units with some - (1→6)-β-D-galactopyranose units and - (1→3)-L-arabinofuranose units.[3] The substitution of numerous OH groups with carboxymethyl groups occurred during the conversion of NAP to CMAP. In the reaction, the hydroxyl groups in NAP were deprotonated by sodium hydroxide, forming alkoxides. Afterward, carboxymethyl groups were formed by reacting NAP-alkoxides with monochloroacetic acid.[18] The overall reaction is given by:

$$NAP\text{-}OH + NaOH \rightarrow NAP\text{-}ONa + H_2O \quad (3)$$

$$NAP\text{-}ONa + ClCH_2{-}COO^- Na^+ \rightarrow NAP\text{-}OCH_2{-}COO^- Na^+ + NaCl \quad (4)$$

At the bulk liquid phase, a side chain reaction occurred simultaneously with the formation of sodium-glycolate from monochloroacetic acid and sodium hydroxide.[18]

$$NaOH + ClCH_2COONa \rightarrow HOCH_2COONa + NaCl \quad (5)$$

A degree of substitution (D_S) indicates the extent of carboxymethylation in a compound. D_S indicates the average number of substituted carboxymethyl groups per anhydroglucose unit.[19] The values of D_S for different CMAP batches are shown in Table 2. The range of D_S was determined to be 0.38-0.51.

FTIR Spectrum Analysis

The conversion of NAP to CMAP was substantiated from FTIR, DSC, Solid-state ^{13}C-NMR, and XRD analysis. The FTIR spectra (4000–400 cm^{-1}) of NAP and CMAP are shown in (Figure 1) which exhibited the absorption in bands at 3449, 3420, 2927, 2925, 1620, 1615, and 1070 cm^{-1}, which are typical bands for carbohydrates.[20] Near 3449 cm^{-1} a strong O−H stretching band of the hydroxyl group [21] was observed in NAP (Figure 1a) due to the involvement of hydrogen bonds of the hydroxyl groups. For CMAP, this O−H stretching band was shifted with reduced intensity of the absorption (Figure 1b) which might indicate the breakage of hydrogen bonds in the carboxymethylation reaction.[22] Figure 1b depicts the characteristic bands of CMAP, which appear at 1610 to 370 cm^{-1}, indicating carboxymethylation. The broad peak at 1420 cm^{-1} of CMAP was mainly attributed to C=O stretching of acid. The band at 2927 cm-^{1} is the indication of $-CH_2-$ groups. Although the bands at 1620, 1615 cm^{-1} are largely belong to C=O stretching. Many −C−−O−−C− groups have peaks in the 950 to 1100 cm^{-1} range that may also indicate the presence of β- and α- linkages in the molecule, respectively.[23]

Differential Scanning Calorimetry (DSC) study

DSC thermograms of NAP and CMAP have been depicted in Figure 2. The NAP exhibited an exothermic event at 73.99°C with a heat flow of 22.38 mW (Figure 2a) that was shifted for CMAP (55.31°C, 20.50 mW) (Figure 2b). In the NAP thermogram (Figure 2a), at around 239°C with a heat flow of 14.15968 mW a melting peak was seen to be intense, while CMAP occurred at 261.5°C with a heat flux of 9.899 mW (Figure 2b). It is likely that the substitution of hydroxyl group protons due to carboxymethylation triggered these variations in endothermic and exothermic behavior, along with heat flow alterations. The extent of carboxymethylation of polysaccharides results in the breaking of intermolecular and intra-molecular hydrogen bonds, as well as the vibrancy of chain segments leads to alteration in the thermal degradation of polymers.[24] However the DSC thermograms of NAP and CMAP indicated good thermal stability.

Solid State ^{13}C-NMR Spectroscopy

^{13}C-NMR spectra of NAP and CMAP are shown in Figure 3. The distinct signals appeared in the NMR spectrum of NAP (Figure 3a) at the respective chemical shifts (δ) 62.229, 72.740, and 103.760 ppm. The peak at 62.229 ppm is attributed to the galactose moiety's (sp^3 hybridization) C-6 carbon, which also indicates the presence of sugar ring carbon with hydroxyl group function. On the other side, the peak at δ = 72.740 ppm inflated at 82 ppm due to signals of C-2, C-3, and C-4 β-carbon atoms.[25] In addition, the peak at δ=76.671 ppm indicates the presence of β-carbon at pyranose ring closure. The signal for the C-3 carbon atom of galactose has appeared as a small bulge at 82.738 ppm.[26] However, that peak at 82.738 ppm was also attributed to the presence of carbon at the furanose ring closure of α-anomers. A peak at δ = 99.316 ppm was detected

Table 2: Different batches of CMAP

Batch no.	*Volume of 0.5N sodium Hydroxide (mL)*	*Volume of 0.4N hydrochloric acid (mL) consumed*	*A**	*D_S***	*SEM*** (statistical significance of 5%) (n = 3)*
P1	5	6.2	3.5	0.41	± 0.0492
P2	5	6.1	3.5	0.51	± 0.0491
P3	5	6.3	3.22	0.38	± 0.0484
P4	5	6.2	3.225	0.41	± 0.0469
P5	5	6.2	3.225	0.41	± 0.0298
P6	5	6.3	3.22	0.38	± 0.0343

* Milliequivalents of NaOH required per gram of sample; ** Degree of substitution; *** Standard error of mean.

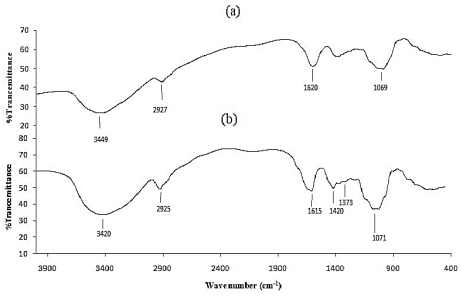

Figure 1: FTIR spectra (a) NAP, (b) CMAP

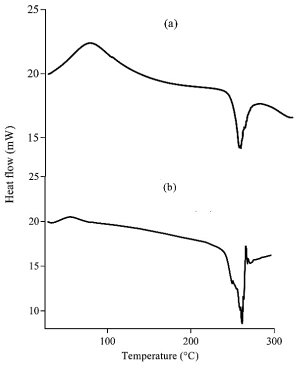

Figure 2: DSC thermogram (a) NAP (b) CMAP

due to the signal from β-anomeric carbon (C-1). Another intense peak observed at δ = 103.760 ppm is due to arabinose's carbon (C-1).[27] In the case of CMAP, the spectra showed the appearance of an additional sharp peak at 177.252 ppm compared to NAP, explicitly the presence of carbonyl carbon of carboxymethyl group at 3-O- position (Figure 3b). Due to both sp^2 hybridizations for carbonyl carbon, the ^{13}C-NMR signal appears the utmost downfield (170–220 ppm).[28] The peak of absorption at 177.252 ppm also indicates the presence of exocyclic carboxyl groups. From the NMR data, the success of carboxymethylation on NAP could be assured. However, the spectral comparison (Figures 3 a and b) revealed the differentiation between NAP and CMAP

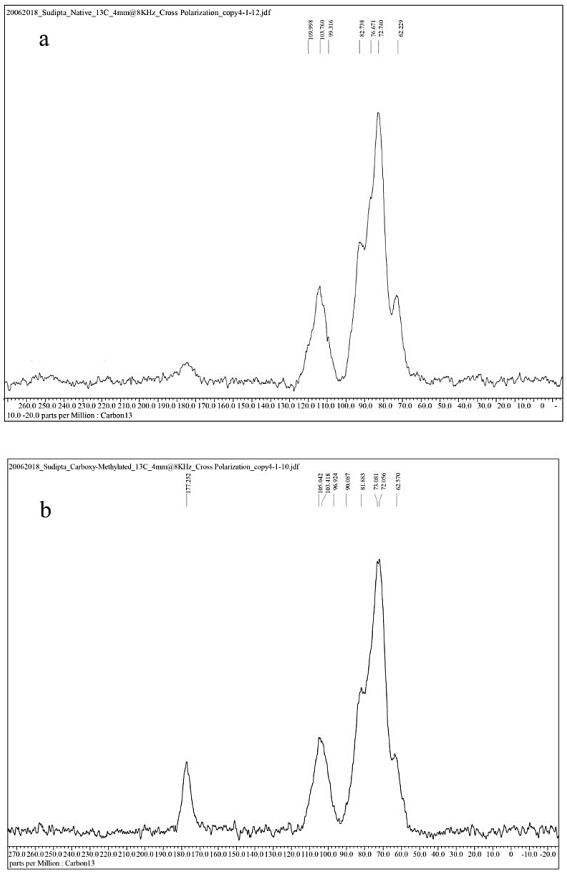

Figure 3: Solid state ^{13}C NMR spectrum of (a) NAP, (b) CMAP

X-ray Diffractometry

An XRD of NAP is in Figure 4a, illustrating its amorphous nature. CMAP exhibits characteristic patterns in XRD at 2θ of 15.250−56.500° (Figure 4b). Moreover, the major sharp and intense patterns at about 2θ of 31.700° (369 cps) and 45.450° (134 cps) indicate the possible crystallinity of NAP on carboxymethylation.[29]

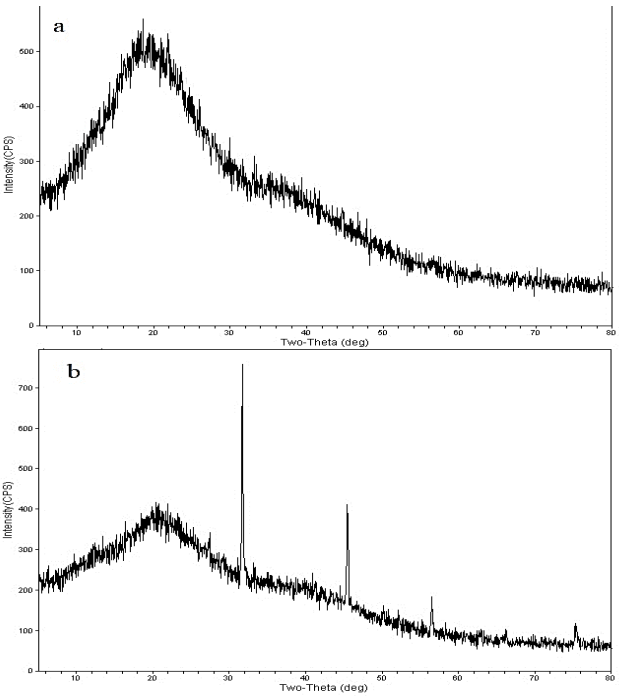

Figure 4: XRD patterns of (a) NAP and (b) CMAP

Zeta Potential Measurements

The zeta potential is the electro-kinetic potential in the interfacial bilayer at the slip plane that separates the mobile fluid from the surface-clinging fluid.[30, 31] The zeta potential of NAP and CMAP were -0.944 and -15.40 mV, respectively (Figure 5a and b). Because of the presence of anions on the carboxymethyl groups (- OCH_2-COO^-), CMAP had a lower zeta potential. (Figure 5b). The zeta potential decreased as the

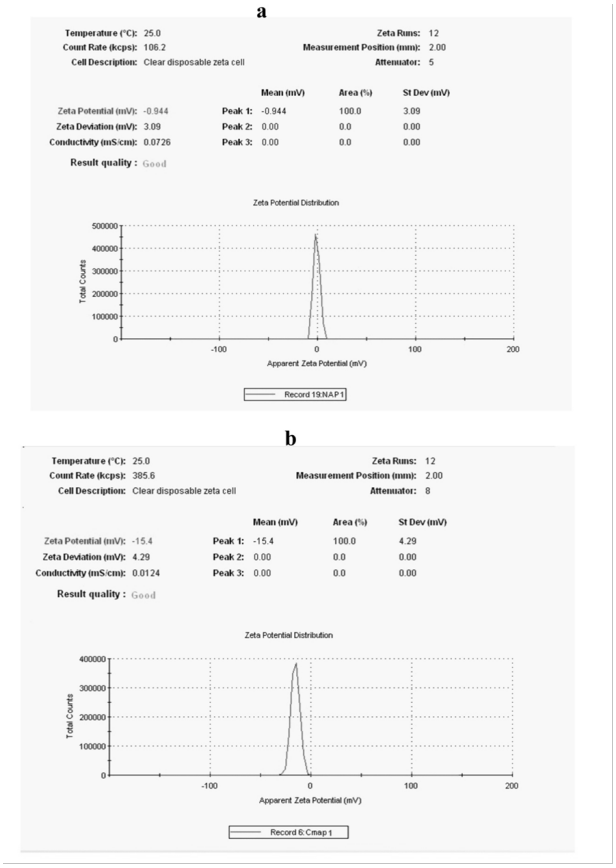

Figure 5: Zeta potential of (a) NAP, and (b) CMAP

D_S increased, showing that CMAP had more carboxymethyl groups and a stronger coulombic repulsion (Table 3). The zeta potential in the NAP samples did not exhibit any notable differences.

Rheological Characteristics

Rheology could be used as a method to evaluate parameters that aid in determining a material's mechanical strength, deformation, and flow properties.[32, 33] The comparative study of the rheological parameters like flow curves, amplitude sweep, frequency sweep, and damping factor of NAP and CMAP (5% w/v) samples reflect the changes in structural integrity, flow behavior due to carboxymethylation.

Dynamic rotational study

The flow curves at variable shear rates are shown in Figure 6 (a-c). There is also a depiction of the viscosity profile of polymers at various pH levels in the Figures. 6d and e. In response to increases in shear rate, the viscosity of the NAP matrix was observed to decline. In addition, it was also found that the NAP matrices exhibited non-Newtonian behavior with the pseudo-plastic flow. In this case, the disentanglement of polymeric chains occurs at a faster rate than the new entanglement formation.[34] There was an observation in Figure 6(a) that, the NAP matrices exhibited higher viscosity (1420 Pa.s for NAP-W, 559 Pa.s for NAP-A, and 115 Pa.s for NAP-B) at a low shear rate (0.01290 S^{-1}). Additionally, the

Table 3: Zeta potential of different batches of CMAP

Batch no. of CMAP	*D_S**	*Zeta potential of CMAP (mV)*	*Zeta potential of NAP (mV)*
P1	0.41	-14.53	-0.944
P2	0.51	-15.40	
P3	0.38	-13.76	
P4	0.41	-14.91	
P5	0.41	-15.03	
P6	0.38	-12.17	

* Degree of substitution

rheogram demonstrated that NAP at neutral pH (NAP-W) displayed greater viscosity than NAP at pH 1.2 (NAP-A); however, the viscosity of NAP-A was higher than the NAP at pH 6.8 (NAP-B).

Flow curves of CMAP matrices also indicated shear-thinning behaviour however; they exhibited much lower viscosities than NAP matrices (Figure 6). There has been an explanation for the increased degree of molecular chain entanglement with concentration attributed to an increase in the viscosity of polymers.[35] Since carboxymethyl groups ($-OCH_2-COO^-$) in CMAP contain anions, the chain segments are electrostatically repellent, preventing entanglements. Due to lack of entanglement, the viscosity of CMAP became lower than NAP matrices. The viscosity of CMAP-A (at pH 1.2) matrix was found to be higher than CMAP-W (at pH 7) and significantly higher than CMAP-B (Figure 6e). The functional groups get ionized at pH 6.8, and the repulsive force becomes strong, which leads to disentanglement and a decrease in viscosity.[36, 37]A shift in the molecular arrangements of the polysaccharide chains in buffer solution has been connected to the decreased viscosity of some ionic polymers with rising solution pH.[38, 39]

According to the flow curve model analysis, the Carreau-Yasuda model best fitted to NAP-W as it displayed a short Newtonian plateau for low shear rates (0.022–0.045 S^{-1}). However, the cross model provided the best fit with NAP-A, and the Ellis model with NAP-B represented pseudo-plastic flow. As for CMAP, the Ellis model effectively fitted samples at all pH values, where the shear stress roughly coincides with half of the final asymptotic viscosity.[40]

Dynamic Oscillatory Studies

Amplitude sweep

The linear viscoelastic region (LVE) is the region in which stress varies linearly with strain for the sample under study.[41] The storage modulus (G') (Pa) is an elastic response of a viscoelastic material that stored the deformation energy subjected to measure during shear.[42] While the loss modulus (G") (Pa) evaluates the deformation energy used by a viscoelastic material during shear, it is the viscous part of the material.

During the amplitude sweep, the amplitude of the deformation is varied with strain (%) at a constant frequency (Rad/sec).[43]

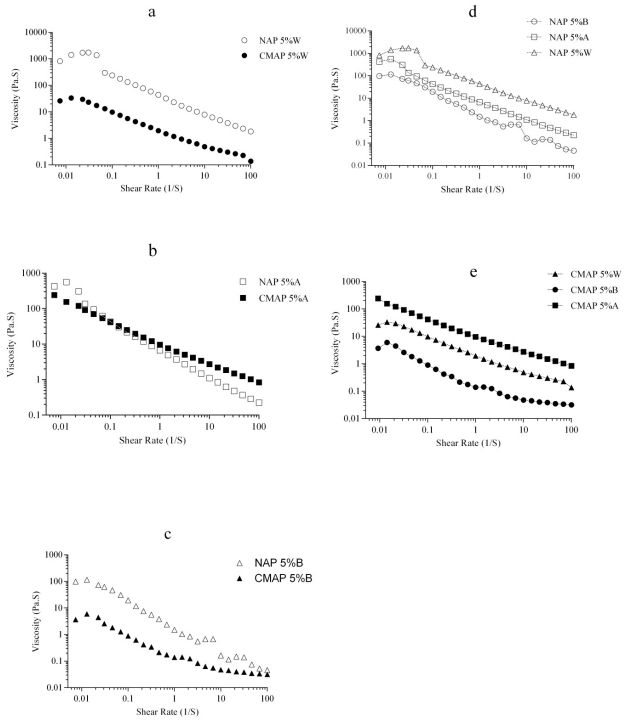

Figure 6: Flow curves (a) in water, (b) at pH 1.2 (c) at pH 6.8; viscosity profile of (d) NAP in water (△), at pH 1.2 (□), at pH 6.8 (○), (e) CMAP in water (▲), at pH 1.2 (■), at pH 6.8(●)

An illustration of the strain sweep results for each matrix (NAP and CMAP) is presented in Figure 7 (a-c). G' and G" in the amplitude curves were dependent on strain amplitude, and the LVE range was derived from these curves. Upon reaching a critical strain of 10%, LVE had been achieved, and G' values were found to be linear up to that point. Beyond the LVE the declination of G' indicated the occurrence of structural deformation. The critical strain refers to the mechanical strength of polymer and the amount of stress at which NAP and CMAP withstand before structural breakdown. IN ALL CASES, the LVE range and G' values of NAP were greater than CMAP (Figure 7 a-c). The overall critical strain of NAP (1–1.5%) was also found to be higher than CMAP (0.01–0.03%). The electrostatic repulsion between the chains of CMAP disrupted entanglements results in low mechanical strength and shorter LVE.

Frequency sweep

During the frequency sweep, the amplitude of the deformation is retained within the LVE, while the angular frequency (ω) is varied.[44] Variable oscillation frequencies make it possible to determine with greater precision the structural integrity, deformity, and rheological stability of a material. The higher values of G' over the G" (G'>G") indicate an elastic structure of material could be said to have a solid viscoelastic nature, while G">G' impart the viscous behavior of the material could be said to have a viscoelastic.[42] The crossover point refers to the transition point at which the value of G' and G" remains the same. For material, if G' is higher than G" before the crossover,

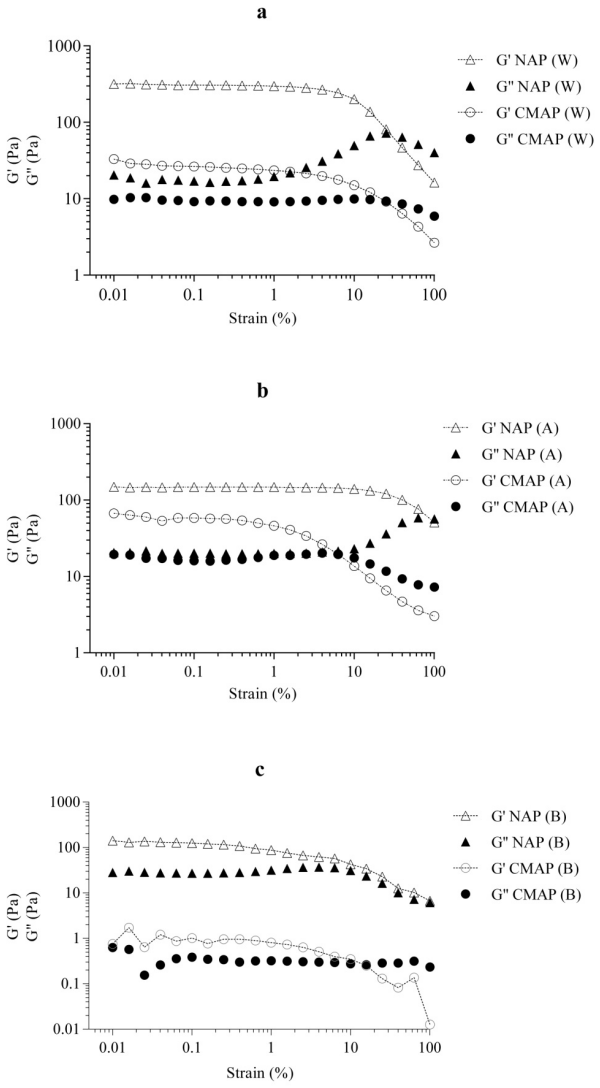

Figure 7: Amplitude sweep (a) in water, (b) at pH 1.2 (c) at pH 6.8

the crossover point could be considered a deformation point. On the other hand, G">G' remains before the crossover then it corresponds to a gel point.[45] The higher differences between G' and G" without crossing each other indicate the more rheological stability of a material.

The frequency sweep analysis was conducted on NAP and CMAP solutions as shown in Figure 8 a-c. Based on the frequency sweep curve, it was observed that G' for NAP is much higher than G" (G'>G") in water and is also rheologically stable (Figure 8a). The values of G' for CMAP in water were also higher than G" but in comparison to NAP, it was much less. At pH 1.2, NAP and CMAP were found to be stable and remain gel-like consistency, although G' values of NAP-A were lower than NAP-W (Figure 8b). In case of CMAP at pH 1.2, the G' values were drastically higher than CMAP in water. However, both polymers were structurally deformed at pH 6.8 (Figure 8c), as they have shown crossover points (NAP at 15.8 Rad/sec, CMAP at 25 Rad/sec). The appearance of

any crossover region indicated the transformation of gel to sol. Moreover, the frequency sweep results indicated that NAP in water formed high entanglements and behaved as a strong viscoelastic gel than acidic pH. While at pH 6.8, the entanglements became weak. In contrast, CMAP at acidic pH has shown gel-like behavior, and ultimately, at pH 6.8, it lost its elastic energy and exhibited a weak gel with a disentangled structure. As the pH of the solution increased, there is a possibility that the functional groups (-COOH-) of CMAP would be ionized, leading to electrostatic repulsion and, thus an increase in molecular dimension and a decrease in entanglements.[46, 47] However, there is also the possibility that the polymer chains would be de-polymerized as the pH rose.[48] Moreover, throughout the frequency sweep study, it has also been noted that in all cases, G' values of NAP were always higher than CMAP.

Damping factor

The inclusion of a damping function in the modeling of polymer melts is crucial to gaining an understanding of nonlinear viscoelasticity.[49] The damping factor is the loss tangent (*tanδ* = G"/G') that measures the internal frictions of materials. The value of loss tangent (*tanδ)* for different viscoelasticity functions[50] is as follows:

tanδ=0: The material is ideally elastic
tanδ=100: The material is ideally viscous
tanδ>1: material is more viscous than elastic
tanδ<1: material is more elastic than viscous
tanδ=1: material is viscoelastic

An investigation of the physical interpretation of the damping function based on experimental results for NAP and CMAP at different pH levels was conducted. From Figure 9, the loss tangents (tanδ) for NAP -W and CMAP-W were less than 1, but the mean tanδ value for CMAP-W (0.56) was higher than NAP -W (0.16). Thus, NAP was more elastic in water than CMAP. Similarly, both polymers showed elastic deformation at pH 1.2. CMAP (*tanδ=0.45) at this pH* was a little more elastic than CMAP-W, while NAP at pH 1.2 (*tanδ=0.59)* remained less elastic than NAP-W. Moreover, both polymers were viscous at pH 6.8 as the loss tangents (tanδ) were more than 1.

Drug-polymer DSC compatibility study

DSC studies are useful tools for assessing the interaction between a drug and an excipient. The melting points of MET and the physical mixture with NAP and CMAP are presented in Table 4. It has been found that the melting point of MET in each of the polymer mixtures is similar to its reported values, [51,] despite some minor reductions in endothermic peak intensity. According to the results, there is no interaction between the excipients and the polymers.

Characterizations of matrix tablets

The average weight of randomly selected matrix tablets containing MET from each formulation of NAP was 1121.5 mg ± 0.04. In contrast, the average weight of the matrix tablets from CMAP formulations containing MET was 1118.7 mg ± 0.05.

The average hardness of all the tablets were about 53.94 Newton ± 0.02 and friability was less than 1%.

A random sample of matrix tablets from each formulation of NAP containing MET was found to be uniform and ranged from 96.89% ± 0.04 to 101.53% ± 0.03. Similarly, the drug content of CMAP tablets was found to be 95.63% ± 0.12 to 107.37% ± 0.06.

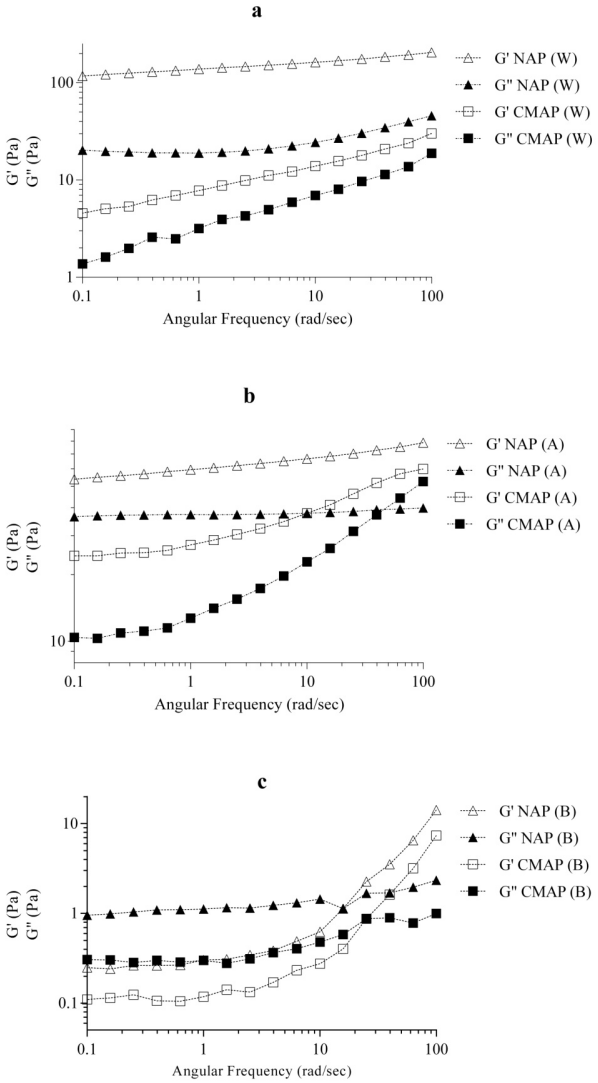

Figure 8: Frequency sweep (a) in water, (b) at pH 1.2, (c) at pH 6.8

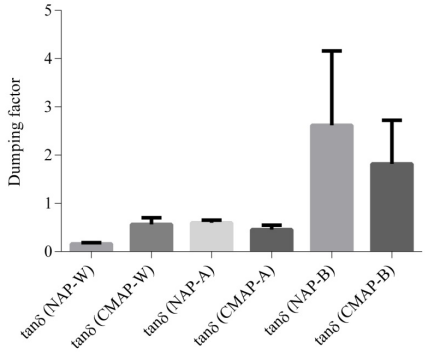

Figure 9: Damping factor of NAP and CMAP

Table 4: Melting point of MET in polymer mixtures from DSC endotherm data

Drug and mixtures	*Melting point (◦C)*
MET	222.37◦C
MET + Physical mixture of NAP	221.63◦C
MET + Powdered tablet of NAP	221.63◦C
MET + Physical mixture of CMAP	221.22◦C
MET + Powdered tablet of CMAP	222.05◦C

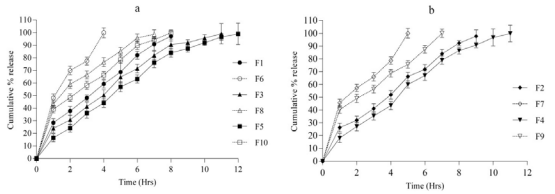

Figure 10: Drug release profiles of MET from NAP (—) and CMAP (- - -) matrix tablets. (a) NAP formulations: F1 (●), F3 (▲), F5 (■); CMAP formulations: F6 (○), F8 (Δ), F10 (□); (b) NAP formulations: F2 (♦), F4 (▼); CMAP formulations: F7 (◊), F9 (▽)

Table 5: AUC of drug release

Medium	*AUC of drug release from NAP matrix (% mg hrs.)*					*AUC of drug release from CMAP matrix (% mg hrs.)*				
	F1	*F2*	*F3*	*F4*	*F5*	*F6*	*F7*	*F8*	*F9*	*F10*
In acid (pH 1.2)	47.44 ± 4.9	42.33 ± 4.7	39.32 ± 3.8	31.63 ± 4.1	28.59 ± 3.3	83.15 ± 2.4	74.24 ± 5.2	72.81 ± 4.3	64.82 ± 4.5	63.46 ± 4.2
In buffer (pH 6.8)	463.95 ± 3.9	514.4 ± 4.1	692.67 ± 3.8	653.44 ± 4.9	726.63 ± 4.6	245.57 ± 5.1	297.53 ± 4.2	476.01 ± 3.8	427.51 ± 4.6	524.88 ± 5. 3

Comparison of drug release

The linearity of the standard calibration curve of MET was determined with a correlation coefficient (R^2) over 0.998 and then used to calculate the amount of drug dissolved in each sample. A comparison of the in vitro drug release from NAP and CMAP matrix tablets is presented in Figure. 10.

The highest amount of MET release in 12 hours from NAP formulation (F5) was 98.81%, while all CMAP tablets showed maximal release before 12 hours. From the entire release profiles of MET (Figure. 10 a and b), it was noted that NAP formulations showed prolonged release and became more sustained as the polymer concentration increased, while CMAP formulations, the release profile showed faster drug release. A "t"-test was used to analyze the data on drug releases from the two matrices. Thus, a statistically significant difference in drug release from NAP and CMAP matrices was observed (p=0.05).

Calculation of AUC was carried out using a linear trapezoidal rule. The calculated values of AUC of drug release (% mg hrs.) from formulations are shown in Table 5.

In CMAP tablets, predominantly drug was released from the gel-like structure owing to a lower viscosity and dis-entanglement than in NAP tablets. The weak gel networks in CMAP matrices are attributed to their low viscosity and loose entanglement structure. While, the strong gel-like structure of NAP and the high viscosity of the compound resulted in a higher degree of entanglement, which resulted in the prolonged release of the drug from tablets containing NAP. The carboxymethylation had changed the structural integrity of CMAP, making it more rheologically unstable than NAP and the rheological behaviors impacted on drug release.[52]

CONCLUSION

An outgrowth of entanglements of the chains in NAP resulted in elastic nature, which imparted structural integrity and higher mechanical strength. Carboxymethylation of NAP significantly altered its rheological properties. A coulombic repulsion between CMAP chains occurs due to the presence of anions within carboxymethyl groups. Therefore, the individual chains of CMAP were unrestricted in their movement, allowing the CMAP structure to disentangle rapidly. NAP and CMAP also exhibit significant differences in their rheological properties at variable pH. While NAP formed a highly entangled structure with higher viscosity at neutral pH, CMAP showed high viscosity at pH 1.2. Thus, such changes also had an impact on the significant change in drug release from matrix tablets. The lack of entanglements and weak gel structures in CMAP made it more prone to erosion.

ACKNOWLEDGMENT

We are grateful for the support the University Grants Commission, New Delhi (DSA Phase-III and UPE-II programs of the UGC) provided. We would also like to extend our gratitude to the Head of the Department of Pharmaceutical Technology at Jadavpur University.

REFERENCES

1. Meena VS, Gupta S. Wood anatomy of Albizia procera correlation between tropical and subtropical from Different geographical zones of Indian subcontinent. Int. J. Sci. Tech. Res. 2014;3(5):1-8.
2. Nguyên NC. Vietnam forest trees. Vietnam forest trees.. 1996.
3. Pachuau L, Lalhlenmawia H, Mazumder B. Characteristics and composition of Albizia procera (Roxb.) Benth gum. Industrial Crops and Products. 2012 Nov 1;40:90-5.
4. Zhang J, Akihisa T, Kurita M, Kikuchi T, Zhu WF, Ye F, Dong ZH, Liu WY, Feng F, Xu J. Melanogenesis-inhibitory and cytotoxic activities of triterpene glycoside constituents from the bark of Albizia procera. Journal of natural products. 2018 Dec 6;81(12):2612-20.
5. Avachat AM, Dash RR, Shrotriya SN. Recent investigations of plant based natural gums, mucilages and resins in novel drug delivery systems. Ind J Pharm Edu Res. 2011 Jan;45(1):86-99.

6. De Paula RC, Santana SA, Rodrigues JF. Composition and rheological properties of Albizia lebbeck gum exudate. Carbohydrate polymers. 2001 Feb 1;44(2):133-9.
7. De Pinto GL, Martínez M, Beltrán O, Rincón F, Clamens C, Igartuburu JM, Guerrero R, Vera A. Characterization of polysaccharides isolated from gums of two Venezuelan specimens of Albizia niopoides var. colombiana. Ciencia. 2002;19:382-7.
8. Gupta MN, Raghava S. Smart systems based on polysaccharides. InNatural-based polymers for biomedical applications 2008 Jan 1 (pp. 129-161). Woodhead Publishing.
9. da Silva MA, Bierhalz AC, Kieckbusch TG. Alginate and pectin composite films crosslinked with Ca2+ ions: Effect of the plasticizer concentration. Carbohydrate polymers. 2009 Jul 19;77(4):736-42.
10. Zhang H, Lamnawar K, Maazouz A. Rheological modeling of the diffusion process and the interphase of symmetrical bilayers based on PVDF and PMMA with varying molecular weights. Rheologica acta. 2012 Aug;51(8):691-711.
11. Münstedt H, Schwarzl FR. Deformation and flow of polymeric materials. Heidelberg, Germany:: Springer; 2014 Nov 18.
12. Caramella C, Ferrari F, Bonferoni MC, Ronchi M, Colombo P. Rheological properties and diffusion dissolution behaviour of hydrophilic polymers. Bollettino Chimico Farmaceutico. 1989 Oct 1;128(10):298-302.
13. Michailova V, Titeva S, Kotsilkova R. Rheological characteristics and diffusion processes in mixed cellulose hydrogel matrices. Journal of drug delivery science and technology. 2005 Jan 1;15(6):443-9.
14. Toğrul H, Arslan N. Production of carboxymethyl cellulose from sugar beet pulp cellulose and rheological behaviour of carboxymethyl cellulose. Carbohydrate Polymers. 2003 Oct 1;54(1):73-82.
15. Barai BK, Singhal RS, Kulkarni PR. Optimization of a process for preparing carboxymethyl cellulose from water hyacinth (Eichornia crassipes). Carbohydrate Polymers. 1997 Mar 1;32(3-4):229-31.
16. Pharmacopoeia I. Vol. II, The Controller Publication. Govt. of India, New Delhi. 2010:1199.
17. Pharmacopoeia I, Volume II. Published by the controller of Publication. Vol. I, New Delhi. 2007;655.
18. Kaity S, Ghosh A. Carboxymethylation of locust bean gum: application in interpenetrating polymer network microspheres for controlled drug delivery. Industrial & engineering chemistry research. 2013 Jul 31;52(30):10033-45.
19. Chakravorty A, Barman G, Mukherjee S, Sa B. Effect of carboxymethylation on rheological and drug release characteristics of locust bean gum matrix tablets. Carbohydrate polymers. 2016 Jun 25;144:50-8.
20. Yuen SN, Choi SM, Phillips DL, Ma CY. Raman and FTIR spectroscopic study of carboxymethylated non-starch polysaccharides. Food chemistry. 2009 Jun 1;114(3):1091-8.
21. Sadalage PS, Pawar KD. Production of microcrystalline cellulose and bacterial nanocellulose through biological valorization of lignocellulosic biomass wastes. Journal of Cleaner Production. 2021 Dec 10;327:129462.
22. Aguir C, M'Henni MF. Experimental study on carboxymethylation of cellulose extracted from Posidonia oceanica. Journal of applied polymer science. 2006 Feb 15;99(4):1808-16.
23. Khondkar P. Composition and partial structure characterization of Tremella polysaccharides. Mycobiology. 2009 Dec 1;37(4):286-94.
24. Gong H, Liu M, Chen J, Han F, Gao C, Zhang B. Synthesis and characterization of carboxymethyl guar gum and rheological properties of its solutions. Carbohydrate polymers. 2012 Apr 15;88(3):1015-22.
25. Yazdani P, Wang B, Rimaz S, Kawi S, Borgna A. Glucose hydrogenolysis over Cu-La2O3/Al2O3: mechanistic insights. Molecular Catalysis. 2019 Apr 1;466:138-45.
26. Agrawal PK, Jain DC, Gupta RK, Thakur RS. Carbon-13 NMR spectroscopy of steroidal sapogenins and steroidal saponins. Phytochemistry. 1985 Oct 29;24(11):2479-96.
27. Chauhan D, Chauhan JS. Flavonoid glycosides from Pongamia pinnata. Pharmaceutical biology. 2002 Jan 1;40(3):171-4.
28. Scholze B, Hanser C, & Meier D. Characterization of the water-insoluble fraction from fast pyrolysis liquids (pyrolytic lignin): Part II. GPC, carbonyl goups, and 13C-NMR. *Journal of Analytical and Applied Pyrolysis*. 2001; *58:* 387-400.
29. Bhatia M, Ahuja M. Psyllium arabinoxylan: Carboxymethylation, characterization and evaluation for nanoparticulate drug delivery. International Journal of Biological Macromolecules. 2015 Jan 1;72:495-501.
30. Liu Y, Lu K, Hu X, Jin Z, Miao M. Structure, properties and potential applications of phytoglycogen and waxy starch subjected to carboxymethylation. Carbohydrate polymers. 2020 Apr 15;234:115908.
31. Ye F, Miao M, Lu K, Jiang B, Li X, Cui SW. Structure and physicochemical properties for modified starch-based nanoparticle from different maize varieties. Food Hydrocolloids. 2017 Jun 1;67:37-44.
32. Isaac VL, Chiari-Andréo BG, Marto JM, Moraes JD, Leone BA, Corrêa MA, Ribeiro HM. Rheology as a tool to predict the release of alpha-lipoic acid from emulsions used for the prevention of skin aging. BioMed Research International. 2015 Dec 16;2015.
33. Kulawik-Pióro A, Ptaszek A, Kruk J. Effective tool for assessment of the quality of barrier creams-relationships between rheological, textural and sensory properties. Regulatory Toxicology and Pharmacology. 2019 Apr 1;103:113-23.
34. Xu X, Xue C, Chang Y, Chen F, Wang J. Conformational and physicochemical properties of fucosylated chondroitin sulfate from sea cucumber Apostichopus japonicus. Carbohydrate polymers. 2016 Nov 5;152:26-32.
35. Mirtič J, Balažic H, Zupančič Š, Kristl J. Effect of solution composition variables on electrospun alginate nanofibers: Response surface analysis. Polymers. 2019 Apr 16;11(4):692.
36. Wang CS, Virgilio N, Carreau PJ, Heuzey MC. Understanding the effect of conformational rigidity on rheological behavior and formation of polysaccharide-based hybrid hydrogels. Biomacromolecules. 2021 Aug 16;22(9):4016-26.
37. Sa B, Mukherjee S, Roy SK. Effect of polymer concentration and solution pH on viscosity affecting integrity of a polysaccharide coat of compression coated tablets. International journal of biological macromolecules. 2019 Mar 15;125:922-30.
38. Boas M, Vasilyev G, Vilensky R, Cohen Y, Zussman E. Structure and rheology of polyelectrolyte complexes in the presence of a hydrogen-bonded co-solvent. Polymers. 2019 Jun 17;11(6):1053.
39. Chen TT, Zhang ZH, Wang ZW, Chen ZL, Ma H, Yan JK. Effects of ultrasound modification at different frequency modes on physicochemical, structural, functional, and biological properties of citrus pectin. Food Hydrocolloids. 2021 Apr 1;113:106484.

40. Al-Behadili A, Sellier M, Hewett JN, Nokes RI, Moyers-Gonzalez M. Identification of Ellis rheological law from free surface velocity. Journal of Non-Newtonian Fluid Mechanics. 2019 Jan 1;263:15-23.
41. Kaboorani A, Blanchet P. Determining the linear viscoelastic region of sugar maple wood by dynamic mechanical analysis. BioResources. 2014 Jan 1;9(3):4392-409.
42. Talens P, Castells ML, Verdú S, Barat JM, Grau R. Flow, viscoelastic and masticatory properties of tailor made thickened pea cream for people with swallowing problems. Journal of Food Engineering. 2021 Mar 1;292:110265.
43. Li C, Liu C, Liu J, Fang L. Correlation between rheological properties, in vitro release, and percutaneous permeation of tetrahydropalmatine. Aaps Pharmscitech. 2011 Sep;12:1002-10.
44. Xiao F, Chen M, Wu S, Amirkhanian SN. A long-term ultraviolet aging effect on rheology of WMA binders. Int. J. Pavement Res. Technol. 2013 Sep 1;6(5):496-504.
45. Rasid IM, Do C, Holten-Andersen N, Olsen BD. Effect of sticker clustering on the dynamics of associative networks. Soft Matter. 2021;17(39):8960-72.
46. Medina-Torres L, Brito-De La Fuente E, Torrestiana-Sanchez B, Katthain R. Rheological properties of the mucilage gum (Opuntia ficus indica). Food hydrocolloids. 2000 Sep 1;14(5):417-24.
47. Yan X, Xiao X, Au C, Mathur S, Huang L, Wang Y, Zhang Z, Zhu Z, Kipper MJ, Tang J, Chen J. Electrospinning nanofibers and nanomembranes for oil/water separation. Journal of Materials Chemistry A. 2021;9(38):21659-84.
48. Achi OK, Okolo NI. The chemical composition and some physical properties of a water-soluble gum from Prosopis africana seeds. International journal of food science & technology. 2004 Apr;39(4):431-6.
49. Rolón-Garrido VH, Wagner MH. The damping function in rheology. Rheologica Acta. 2009 Apr;48:245-84.
50. Wang H, Ke L, Ding Y, Rao P, Xu T, Han H, Zhou J, Ding W, Shang X. Effect of calcium ions on rheological properties and structure of Lycium barbarum L. polysaccharide and its gelation mechanism. Food Hydrocolloids. 2022 Jan 1;122:107079.
51. Gramaglia D, Conway BR, Kett VL, Malcolm RK, Batchelor HK. High speed DSC (hyper-DSC) as a tool to measure the solubility of a drug within a solid or semi-solid matrix. International journal of pharmaceutics. 2005 Sep 14;301(1-2):1-5.
52. Li C, Liu C, Liu J, Fang L. Correlation between rheological properties, in vitro release, and percutaneous permeation of tetrahydropalmatine. Aaps Pharmscitech. 2011 Sep;12:1002-10.